

Program NetMoment; Simultaneous Calculation of Moment, Source Corner Frequency, and Site Specific t^* from Network Recordings

L. Hutchings

December 12, 2001

U.S. Department of Energy

Lawrence
Livermore
National
Laboratory

DISCLAIMER

This document was prepared as an account of work sponsored by an agency of the United States Government. Neither the United States Government nor the University of California nor any of their employees, makes any warranty, express or implied, or assumes any legal liability or responsibility for the accuracy, completeness, or usefulness of any information, apparatus, product, or process disclosed, or represents that its use would not infringe privately owned rights. Reference herein to any specific commercial product, process, or service by trade name, trademark, manufacturer, or otherwise, does not necessarily constitute or imply its endorsement, recommendation, or favoring by the United States Government or the University of California. The views and opinions of authors expressed herein do not necessarily state or reflect those of the United States Government or the University of California, and shall not be used for advertising or product endorsement purposes.

This work was performed under the auspices of the U. S. Department of Energy by the University of California, Lawrence Livermore National Laboratory under Contract No. W-7405-Eng-48.

This report has been reproduced directly from the best available copy.

Available electronically at <http://www.doe.gov/bridge>

Available for a processing fee to U.S. Department of Energy
and its contractors in paper from

U.S. Department of Energy
Office of Scientific and Technical Information
P.O. Box 62
Oak Ridge, TN 37831-0062
Telephone: (865) 576-8401
Facsimile: (865) 576-5728
E-mail: reports@adonis.osti.gov

Available for the sale to the public from
U.S. Department of Commerce

National Technical Information Service
5285 Port Royal Road
Springfield, VA 22161
Telephone: (800) 553-6847
Facsimile: (703) 605-6900

E-mail: orders@ntis.fedworld.gov

Online ordering: <http://www.ntis.gov/ordering.htm>

OR

Lawrence Livermore National Laboratory
Technical Information Department's Digital Library
<http://www.llnl.gov/tid/Library.html>

**Program NetMoment; Simultaneous Calculation of Moment, Source Corner
Frequency, and Site Specific t^* from Network Recordings**

Lawrence Hutchings

Lawrence Livermore National Laboratory
Hazard Mitigation Center
P.O. Box 808
Livermore, California 94551

UC/LLNL Campus/Laboratory Collaboration Project

December 12, 2001

Introduction

The purpose of computer program NetMoment (Appendix I) is to utilize fundamental knowledge of earthquake sources, propagation attenuation, and site response in a simultaneous inversion of network data to determine the moment and source corner frequency of earthquakes, and site specific t^* . The source parameters are especially difficult to determine for small earthquakes.

A fundamental problem in determining the source corner frequencies of small earthquakes is that site response can result in spectral corner frequencies in the range that may be expected from the earthquakes themselves. Several authors have identified this as f_{max} (Hanks, 1982), a constant corner frequency for small events so that below a threshold moment (about 1.0×10^{21} dyne-cm) the corner frequency remains constant as the size of events diminishes. Hutchings and Wu (1990) found that for the southern California region, events with moment less than about 1.5×10^{21} dyne-cm (about magnitude 3.4) show no source effect in their spectra. Hanks (1982) found the threshold to be about 1.0×10^{21} dyne-cm for other southern California sites. Baise et al. (2002) found borehole recordings on Yerba Buena Island, in San Francisco Bay, to have corner frequencies limited to about 3-5 Hz for $M < 4.0$ earthquakes in the region. Some authors have attributed this to a minimum source dimension for earthquakes, which results in a decrease in stress drop for smaller events (Archuleta et al., 1982; Papageorgiou and Aki, 1983). An alternative explanation is that the constant corner frequencies result from whole path or near site attenuation and/or amplifications due to soil response. This is supported by a wide body of literature (Anderson and Hough, 1984; Hutchings and Wu, 1990; Blakeslee and Malin, 1991; Aster and Shearer, 1991; Abercrombie, 1995). Abercrombie, for example, estimated source corner frequencies from events recorded in granite at a depth of 2.5 Km in the Cajon Pass scientific drill hole and observed corner frequencies about a factor of 10 higher than observed at the surface.

An interesting question regarding f_{max} is that if there is a spectral fall-off due to attenuation and an apparent source corner frequency in the spectra, then there should be an additional fall-off at frequencies above the actual source corner frequency (Jarpe et al., 1989). A Brune source model with 100 bar stress drop predicts a source corner frequency of 6.0 Hz and 15 Hz for events with moment of 1.0×10^{21} and 1.0×10^{20} dyne-cm, respectively (about magnitude 3.2 and 2.2, respectively). If source corner frequencies are not observed, then this suggests that stress drops are higher than 100 bars. Wennerberg has attempted spectral division with empirical Green's functions to try to identify the actual source corner frequency of larger events and was not able to (Wennerberg, 1983). One aspect of program NetMoment is that it attempts to find both the spectral fall-off due to attenuation and the source spectral shape (source corner frequency) in observed spectra.

Knowing the corner frequency of source events for empirical Green's functions is important when synthesizing ground motion because most empirical Green's function approaches assume that corner frequencies of source events are known. Hutchings and Wu (1990) assume that source events are small enough that the events are effectively

impulsive point sources, so that their corner frequencies should be higher than the highest frequency to be modeled. If source events have corner frequencies that are known, then a source model (i.e. Brune source) can be used to deconvolve out a source spectral shape from the EGF's to create effective impulsive point source events.

The moment of small events is also difficult to determine because records are usually band limited by cultural noise to about 0.5 Hz, and at this frequency range the site response and near surface propagation path Q effects on spectra can be significant. However, knowing the moment of local earthquakes provides a valuable comparison of relative earthquake size, and is essential to estimate stress drop. Also, knowing the moment of source events used in strong ground motion synthesis with empirical Green's functions is critical to the predictive capability for strong ground motion because amplitudes of synthesized accelerograms are linearly dependent upon their moment estimate. Approaches such as Irikura (1994), Hutchings and Wu (1990) and most other approaches (see Joyner and Boore, 1982), add up or scale empirical Green's functions based upon the moment estimate of the small events.

If moments are calculated from long period spectral levels that are affected by site response, then inaccurate values will be estimated. Kasameyer and Jarpe (1996) and Bonilla et al. (1997) showed that site response is significant for frequencies at least to 0.5 Hz for soil sites. However, usually the moment that is calculated is one that is an average of all moments estimated. This can be dealt with by weighting the moment estimates, so that hard rock sites that are less likely to be affected by site response are given more weight when determining moments. However, the bias introduced by site response when determining moments of small earthquakes needs more research.

Theory

The joint inversion is based upon the assumption that corrected long period spectral levels and the source corner frequencies from a particular earthquake will have the same value at each site, so that differences in spectra are due to propagation path and individual site t^* . t^* is $R/(QV)$ and is raised to the negative power of the exponent to model attenuation as $\exp(-\pi f t^*)$. R is distance traveled, V is velocity, and Q is the seismic quality factor. We corrected spectra for whole path t_r^* and solved for site specific t_g^* .

Anderson and Hough (1984) showed that to a first approximation attenuation could be separated into a near-surface attenuation and an attenuation at depth. Our assumption is that whole path attenuation is fairly uniform and determined from the velocity model. We also assume that VQ near a site will vary with individual site conditions. It is well known, for example, that poorly consolidated materials have low velocities and low Q values, and thus would have high t_g^* values. Similarly, rock has high velocity and high Q values and would have low t_g^* values. Of course, we cannot identify what is specifically contributing to t_g^* and over what distance range. In particular, there is a trade-off

between t_r^* and t_g^* . Here, we use t_r^* to normalize for propagation distance and examine relative values of t_g^* . We assume that to a first order Q and thus t^* is frequency independent. This is supported by observations to calculate Q in the shallow crust (Hough et al., 1988; Frankel and Wennerberg, 1989).

We used a nonlinear least squares best fit of displacement spectra of the S-wave energy of the recorded seismograms to the Brune source model to solve for our free parameters. The Fourier amplitude spectra of recorded seismograms were corrected to represent moment at the long period asymptote and for whole path attenuation. They were then fit to the Brune (1972) displacement spectral shape with site specific t^* and moment as the long period spectral asymptote. Spectra were fit to the modified Brune spectra:

$$(1) \quad \Omega(f) = \frac{M_o \exp(-\pi f t_g^*)}{\left[1 + \left(\frac{f}{f_c}\right)^2\right]}$$

where M_o is the moment, f is frequency, f_c is the source corner frequency, and t_g^* is site specific t^* . The best fitting combination of free parameters (M_o, f_c, t_g^*) was found by iteration from a starting model using the Simplex algorithm (Caccecchi and Cacheris, 1984; Nelder and Mead, 1965; Numerical Recipes, 1998, Chapter 10.4).

The correction to spectra prior to the joint inversion is based upon the equation for moment from Aki and Richards (1980, pg. 116). Spectra of recorded seismograms were corrected by:

$$(2) \quad \Omega'(f) = \frac{4\pi R \rho_x^{1/2} \rho_\zeta^{1/2} \beta_x^{1/2} \beta_\zeta^{5/2}}{S^S F^S} U(f) \exp(\pi f t_r^*)$$

where $U(f)$ is the recorded displacement spectra, t_r^* is whole path t^* , R is correction for geometrical spreading, ρ_x is density at the station and ρ_ζ is density at the source, β_x is shear velocity at the station and β_ζ is shear velocity at the source. S and F are the free surface correction and focal mechanism correction, respectively. The free surface correction is determined from the velocity model using the reflection coefficients as outlined in Aki and Richards (1980, pg. 190). The focal mechanism correction is determined by the radiation pattern as outlined by Aki and Richards (1980, pg. 115), $\Omega'(f \rightarrow 0) = M_o$.

Application to Athens

The 7 September 1999, $M_w=5.9$ Athens earthquake is the first moderate-to-strong earthquake ever reported to have occurred at such a small distance (20 km) from the historical center of the city. Officials reported that about 100 buildings collapsed, which caused 143 casualties. The National Observatory of Athens, Institute of Geodynamics (NOAIG) recorded the main earthquake and aftershocks at several locations in the metropolitan area (Kalogeras and Stavrakakis, 1999), and the University of Athens, Department of Geophysics-Geothermics (UoADGG) recorded aftershocks in many locations where damage was significant (Papadimitriou et al., 2000). Figure 1 shows the morphology of the Athens area, the epicenter of the main shock, and locations of stations used in this study. The results discussed here were previously published in (Ioannidou et al., 2002).

Weak motion recordings were obtained from aftershocks at a wide range of distances from 9 to 52 km. NOAIG data were recorded by their permanent strong motion array and Attico Metro S. A. instruments. The procedure for processing strong motion records of NOAIG is based on the standard procedure of the CALTECH Institute (Trifunac and Lee, 1973), and is described, in detail, by Stavrakakis et al. (1993). The instrument correction used is that described by many investigators (Hudson & Brady, 1971; Trifunac & Lee, 1973; Trifunac et al., 1973; Hudson, 1979; Trifunac & Lee, 1979), while values of Ormsby filters proposed by Basili & Brady (1978) and used by previous authors for processing strong motion records in Greece (Carydis et al., 1984; Margaris, 1986; Anagnostopoulos et al., 1986; Carydis et al., 1989; Makropoulos et al., 1989; Lekidis et al., 1991), are applied.

The UoADGG deployed two types of stations during the installation of the temporary network. Acceleration was recorded at sites PEFK and COUR, situated within the center of the network, using Kinematics ETNA instruments. The previously mentioned procedure for processing strong motion accelerometer records was applied on the data from these stations. At the NEOK, STEF, MAGO, FILI, PSAR and ZOFR sites RefTec recording instruments were installed. The first four of these were equipped with the LE-3D 1 Hz Lennartz sensor while the last two stations were connected to GURALP CMG 40-T broadband seismometers. The records obtained were instrument response corrected according to the sensor specifications to obtained velocity time histories.

Table 3 lists source information for the events used in this study. Hypocentral locations for the main event and many of the aftershocks were obtained from Papadopoulos et al. (2000) (indicated by an * in Table 3). Locations for the events shortly after the main event (indicated by a + in Table 3), which were not recorded by temporary local networks, were obtained using information from the permanent networks in Greece and s-p arrival time intervals from the strong ground motion records (Kalogeras and Stavrakakis, 1999). Focal mechanism solutions were obtained from Papadopoulos et al. (2000). In addition, several events were located and focal mechanism solutions were

obtained by combining data from NOAAIG with that from the UoADGG. These are identified by ++ in Table 3. These hypocentral solutions are consistent with other solutions obtained in this study. Since these solutions used a different station distribution, and a slightly varied velocity model, this gives confidence that the locations of events used in this study are near the limit of accuracy that can be achieved for this area. The focal mechanism solutions from the combined data are close to that of the main event, as are many of the events listed in Table 3 from Papadopoulos et al. (2000). Table 4 lists the stations used in the inversion and Figure 9 shows a plot of their locations along with the location of the source event.

Analysis

The focal mechanism correction is determined by the radiation pattern as outlined by Aki and Richards (1980, pg. 115), and discussed further below. Density is determined from the shear wave velocity by the linear relation: $\rho = (\beta - 0.35)/1.88$ (Lama and Vutukuri, 1978). $\Omega'(f \rightarrow 0) = M_0$. Ten seconds of S arrivals were used in the calculation. We are using Q_s for whole path t^* since only S-waves are used in the inversion. Seismograms were rotated to radial and transverse components, and the vertical and radial were square-of-sum-squared added to get one S_v spectrum, then the S_v and Sh components were corrected for focal mechanism solution. S_v and Sh components were square-of-sum-squared added to get one S-wave spectrum and corrected with the remaining corrections of equation 2 before the inversion. Corrected spectra were fit to equation 1 by fitting frequencies from 1.0 to 20.0 Hz for most aftershocks, and 0.3 to 25.0 Hz for the main event. Some aftershocks had better signal to noise and were fit to 0.5 to 20.0 Hz, and some had worse signal to noise and were fit to 2.0 to 15.0 Hz. These frequency ranges ensured that all recordings were above noise. Table 3 lists the number of aftershocks at each used in the inversion.

Obviously, model parameters are dependent upon the constants used in the equations 1 and 2. We attempted to identify the uncertainty attributed to these constraints. The moment is dependent upon shear velocity to the 4th power. Shear velocity is to the 3rd power in equation 2 and density is determined from the shear velocity from the linear relation: $\rho = (\beta - 0.35)/1.88$ (Lama and Vutukuri, 1978). In equation 2:

$\rho_x = 2.37 \text{ gm/cm}^3$ is the surface density and is based upon near surface basement rock P-wave velocity of 4.1 km/sec. It is assumed that the long period waves used to calculate moment sample primarily the basement structure. ρ_z varies with the depth of the event, $\rho_z = 3.26 \text{ gm/cm}^3$ for the main shock. A difference of 20% in shear velocity results in a change in moment value of about a factor of 2.

There is a fairly significant scatter in long period spectral levels of a factor of up to ± 5 . This may be due to either a difference in site response at low frequencies, an inappropriate correction for focal mechanism solution, directivity effects, hypocentral location, or unidentified long period noise. We excluded significant directivity effects as the

cause because of the size of aftershocks used, and determined that at frequencies between 1.0 and 20.0 the signal to noise ratio was such that noise was not a cause. We also identified that a similar difference in spectral amplitudes as observed at long period spectral levels was evident throughout the frequency range of recording. This suggests that it is due to inappropriate FMS corrections or systematic amplifications. We examined the effect of focal mechanism solution (FMS) correction for amplitude and found that there was a reduction in the scatter if a FMS correction was applied. If a FMS was available, we applied a correction that was limited to a minimum of 0.25 (see Hutchings and Wu, 1990). If a FMS was not available, an average value of 0.63 was used for the FMS radiation pattern correction (Wu and Ben-Menahem, 1965). We could not identify whether site response was a contributing factor. We calculated the standard deviation of the moment calculation for all the events together to be a factor of ± 2.1 .

The fit to t_g^* and f_c are dependent upon the long period spectral level and in a simultaneous inversion this can result in a bias. For example, if a site has a factor of 2 greater long period spectral level than the solution for the joint inversion, and is forced to fit the site specific high frequency, then the t_g^* value will be higher and the f_c will be lower than if spectra were fit individually. Therefore, in an effort to get unbiased value of t_g^* and f_c we normalized spectra to have the same long period spectral level (average of all recordings for a particular event), then conducted the simultaneous inversion. This did not affect the moment calculation significantly because t_g^* generally has minimal effect at these periods and the spectral fit of the inversion is primarily the mean of long period values anyway. This inherently adds the assumption that at the longest periods, site response is not a factor.

There is an obvious trade-off between the t_r^* correction and t_g^* . However, we found essentially no trade-off between source corner frequency and choice of Q_s between 250 and 1000 for t_r^* . We have limited the range for whole path Q_s of between 250 and 500 from previous studies of Q_s and our analysis. Hashida et al. (1988) used macroseismic data and found that an average Q_s ranges between 50 and 1000 for the crust for the whole area of Greece and that the Continental Greece is an area of higher Q_s in the crust than the Aegean area. Papazachos (1992) by using the same kind of data but in a different approach estimated a mean Q_s of 350 ± 140 at around 1 Hz for the same region. Hatzidimitriou et al. (1993) by using acceleration data found Q_s values ranging between 30 and 360 for frequencies 4-10 Hz. We found that a Q_s value of 350 to 500 for whole path Q correction gave the most consistent spectral fall-off at all stations. In particular, lower values of Q_s resulted in an over correction when applied to distant stations, such as THVC and RFNA, and a spectral slope that was lower at higher frequencies. We have used a value of $Q_s = 350$ for t_r^* correction.

Results

Table 1 lists individual t_g^* values obtained from program NetMoment, along with one standard deviation values of those sites that had 4 or more recordings. Table 3 lists the moment and corner frequency obtained for the source events. A reliable moment value was not obtained for the main event because the source corner frequency is near the low frequency recording limit of about 0.5 Hz. Figure 4 shows a plot of calculated t_g^* values at each station. The circle size corresponds to t_g^* values. Figures 5 and 6 show fits of moment, the Brune source model, and t_g^* to corrected spectra for twelve of the events. There are several points that should be noted. First, there is one spectral fit for each spectra plotted, and they all converge to a common asymptotic value, the moment. The spectra are shown only for the frequency range where data is considered adequate for the study, and the asymptotic fit to the Brune source model may have a higher value than is indicated by the plot. Since t_g^* is not allowed to be negative, spectra that have a slope less than the $1/f^2$ of the Brune source model cannot be fit. See, for example, the spectra with shallow slope for event 990907115651, the main event. Spectra such as these will have t_g^* of zero, and are interpreted to have had no t_g^* . It is recognized that a site specific amplification can have this effect, and thus bias results. Generally, spectra show varying slopes of the high frequency fall-off due to t_g^* .

Figure 7 shows the corner frequency values as a function of moment for the events in this study. Also plotted is the corner frequency relationship predicted by a Brune source model with 100 bar stress drop. It is apparent that corner frequencies identified in this study are consistent with those generally described by the Brune source model. Scatter in corner frequencies may be due to variation in stress drop or uncertainties in corner frequency picks. Trial and error calculations for this study shows that corner frequency picks vary by about ± 1 Hz, depending upon choices in calculating the L2 norm.

References

- Abercrombie, Rachael E. (1995) Earthquake source scaling relationships from -1 to 5 M_L using seismograms recorded at 2.5-km depth. *J. Geophys. Res.* **100** 24015 - 24036.
- Aki, K. and P. G. Richards (1980). Quantitative seismology, *Theory and Methods*, Volumes I and II, W. H. Freeman and Company, San Francisco, CA.
- Anderson, J.G. and S. Hough (1984) A model for the shape of the Fourier amplitude spectra of accelerograms at high frequencies. *Bul. Seis. Soc. Am.* **74**, 1969-1994.
- Archuleta, R., F/ Bonilla, M. Doroudian, F. Heuze, P-C. Liu, and J. Steidl (2000) Strong Earthquake Motion Estimates for the UCSB Campus, and Related Response of the Engineering I Building", UC/CLC report.

Baise, Laurie, Lawrence Hutchings, and Steven Glaser (2002) Analysis of Site Response at Yerba Buena Island, San Francisco Bay, California from Weak Motion Recordings. submitted to Special Issue on Site Response, *Bollettino di Geofisica*, Trieste, Italy.

Blakeslee, S. and P. Malin (1991) High-frequency site effects at two Parkfield downhole and surface stations. *Bul. Seis. Soc. Am.* **81**, 332-345.

Bonilla, Luis Fabian, Jamison H. Steidl, Grant T. Lindley, Alexei G. Tumarkin, and Ralph J. Archuleta (1997) Site amplification in the San Fernando valley, CA: variability of the site effect estimation using the S-wave coda, and H/V methods. *Bul. Seis. Soc. Am.* **87**, 710-730.

Brune, J.N. (1971) Tectonic Stress and the Spectra of Seismic Shear Waves from Earthquakes. *J. Geophys. Res.* **75**, 4997-5010 (Correction, *J. Geophys. Res.* **76**(20), 5002, 1972).

Caceci, M.S. and W.P. Cacheris (1984) Fitting curves to data, *Byte Magazine*, May, 340-360.

Carydis, P.G., Drakopoulos, J. and Taflambas, J. (1984). Evaluation of the Corinth strong motion records of February 24 and 25, 1981. Proc. of EAEE, Athens.

Carydis, P.G., Drakopoulos, J., Kalogeras, J., Mouzakis, H., Taflambas, J. and Vougiouka, N. (1989). Analysis of the Kalamata, Greece, strong motion records and correlation with the observed damages. Proc. of XXI General Assembly of E.S.C., 23-27 Aug. 1988, Sofia, Bulgaria, 344-355.

Edaphomihaniki E.P.E., 1998. Geotechnical study of the Thiva area. Ministry of Development, General Secretariat of Research and Technology, Auto-Seismo-Geotech, Vol B, Report 4.1.

EERI. The Athens, Greece Earthquake of September 7, 1999. Special earthquake report - Learning from Earthquakes. November 1999. <http://www.eeri.org/earthquakes/Reconn/Greece1099/Greece1099.html>.

Frankel, A. and L. Wennerberg (1989) Microearthquake spectra from the Anza, California, seismic network: site response and source scaling. *Bull. Seis. Soc. Am.* **79**, 581-609.

Hanks, T.C. (1982) *fmax*. *Bul. Seis. Soc. Am.* **72**, 1867-1879.

Hanks, T.C. and H. Kanamori (1979) A moment magnitude scale. *J. Geophys. Res.* **84**, 2348-2350.

Hashida, T. Stavrakakis, G. and Shimazaki, K. (1988). Three-dimensional seismic attenuation structure beneath the Aegean region and its tectonic implication. *Tectonophysics*, **145**, 43-54.

Hatzidimitriou, P., Papazachos, C., Kiratzi, A. and Theodoulidis, N. (1993). Estimation of attenuation structure and local earthquake magnitude based on acceleration records in Greece. *Tectonophysics*, **217**, 243-254.

Heaton, T.H. (1982) The 1971 San Fernando earthquake: a double event? *Bul. Seis. Soc. Am.* **72**, 2037-2062.

Hough, S.E., J.G. Anderson, J. Brune, F. Vernon III, J. Berger, J. Fletcher, L. Harr, T. Hanks, and L. Barker. Attenuation near Anza, California, *Bull. Seis. Soc. Am.* **78**, 672-691.

Hudson, D.E. (1979). Reading and interpreting strong motion accelerograms. EERI, Pasadena, California, 1-112.

Hudson, D.E. and Brady, A.G. (1971). Strong motion earthquake accelerograms - Digitized & plotted data. Vol. IIA. EERL, 71-50, California Institute of Technology, Pasadena, California.

Hutchings, L. and F. Wu (1990). Empirical Green's functions from small earthquakes—A waveform study of locally recorded aftershocks of the San Fernando earthquake, *J. Geophys. Res.* **95**, 1187–1214.

Ioannidou, Eleni, Ioannis Kalogeras, Nicholas Voulgaris, Lawrence Hutchings, and George Stavrakakis(2002). Analysis of Site Response in the Athens Area from the 7 September 1999, Mw=5.9 Athens Earthquake and Aftershock Recordings, and Intensity Observations. submitted to Special Issue on Site Response, *Bollettino di Geofisica*, Trieste, Italy.

Jarpe, S.P., L.J. Hutchings, T.F. Hauk, and A.F. Shakel (1989) Selected Strong- and Weak-Motion Data from the Loma Prieta Earthquake Sequence. *Seis Res Letters*, **60**, 167-176.

Joyner, W. B. and D. M. Boore (1982) Measurement characterization and prediction of strong ground motion, in *Proc. Earth. Engin. Soil Dyn. II: Recent Advances in Ground Motion Evaluation*, ASCE, park City, Utah, 43-102.

Kalogeras, I.S. and Stavrakakis, G.N. (1999). Processing of the strong motion data from the September 7th, 1999 Athens earthquake. National Observatory of Athens, Geodynamic Institute, Publ. No 10 (CD-ROM).

Katsikatsos, G., G. Migiros, M. Triandaphyllis and A. Mettos (1986) Geological Structure of Internal Hellenides. *Geological and Geophysical Research Special Issue IGME*, pp. 191-212, Athens.

Kouskouna, V., Makropoulos, K., Raftopoulos, D., Malakatas, N., Albini, P., Stucchi, M. and Rubbia, G. (2000) The September 7, 1999, Parnitha earthquake: Macroseismic observations. Abstract in EGU, Sept. 2000, Lisbon, Portugal.

Lachet, C. and P.-Y. Bard (1994) Numerical and Theoretical Investigations on the possibilities of Nakamura's Technique. *Journal of Physics of the Earth*, **42**, 377-397.

Lama, R.D. and V.S. Vutukuri (1978) *Handbook on Mechanical Properties of Rocks*, V II, R.D. Trans Tech Publications, p. 245, pp. 481.

Lekidis, V., K. Pitilakis, V. Margaris, N. Theodoulidis and A. Moutsakis(1991). The Edessa earthquake of Dec. 21, 1991. Report 91-01, Institute of Engineering Seismology and Earthquake Engineering (ITSAK), 1-68.

Lekkas, E. (2001) The Athens earthquake (7 Sept. 1999): intensity distribution and controlling factors, *Engineering Geology* **59** (2001) 297-311.

Lindley, Grant T. and Ralph J. Archuleta (1992) Earthquake Parameters and the Frequency Dependence of Attenuation at Colinga, Mammoth Lakes, and the Santa Cruz Mountains, California. *J. Geophys. Res.* **97**, No. B10, 14137- 14154.

Makropoulos, K., Drakopoulos, J. and Kouskoun, V. (1989). The earthquake sequence in

- Volos, Central Greece, April 30, 1985. Analysis of strong motion. IASPEI, (Abstracts), Istanbul, 1989.
- Margaris, V.N. (1986). Digitizing errors and filters. Report 86-03, Institute of Engineering Seismology and Earthquake Engineering (ITSAK), 1-43.
- Mariolakos, I. and I. Foundoulis (2000) The Athens Earthquake Sept. 7, 1999, the Neotectonic Regime of the Affected Area, Ann. Geol. des Pay Helleniques, Tom. XXXVIII, Fasc. B.
- Nelder, J. A. and R. Mead (1965) A simplex method for function minimization, *Computer J.*, 7, 308.
- Press, William H., Brian P. Flannery, Saul A Teukalsky, and William T. Vetterling (1998) *Numerical Recipes* (1998), Cambridge University Press.
- Papadimitriou, P., G. Kassaras, N. Voulgaris, I. Kassaras, N. Delibasis, and K. Makropoulos (2000) The September 7, 1999 Athens Earthquake Sequence Recorded by the Cornet Network: Preliminary Results of Source Parameters Determination of the Mainshock. Department of Geophysics, University of Athens, 157 84 Athens, Greece.
- Papadopoulos, G.A., G. Drakatos, D. Papanastassiou, I. Kalogeras, G. Stavrakakis (2000) Preliminary Results about the Catastrophic Earthquake of 7 September 1999 in Athens, Greece. *Seis. Res. Let.* 71, No. 3, pp.318-329.
- Papazachos C. (1992). Anisotropic radiation modeling of macroseismic intensities for estimation of the attenuation structure of the upper crust in Greece. *Pageoph*, 138, 445-469.
- Protonotarios I. (1999) Preliminary conclusions from the Sept. 9, 1999 Earthquake. Workshop on The Sept. 9, 1999 Athens Earthquake, November 2, 1999 Athens, Greece
- Rollins, K.M., M.D. Mchood, R.D. Hryciw, and M. Homolka (1994) Ground Response on Treasure Island. *Strong Ground Motion*. pp. A109-A121.
- Stavrakakis, G.N., Kalogeras, I.S. and Drakopoulos, J.C. (1993). Preliminary analysis of Greek accelerograms recorded at stations of NOA's network: Time period 1973 - 1990. Proc. 2nd Congress Hellenic Geophys. Union, Florina, Greece, 5-7 May, 175-191.
- Trifunac, M.D. and Lee, V.W. (1973). Routine computer processing of strong-motion accelerograms. *EERL*, 73-03.
- Trifunac, M.D. and Lee, V.W. (1979). Automatic digitalization and processing of strong-motion accelerograms. Part I. Univ. Southern California, Tech. rep. CE, 79-151.
- Trifunac, M.D., Udawadia, F.E. and Brady, A.G. (1973). Analysis of errors in digitized strong-motion accelerograms. *Bull. Seism. Soc. Am.*, 63,
- Tsamis, 1999. Study for the development and extension of the building of the Nuclear Technology and Radiation Protection Institute. Nuclear Center for Scientific Research "Demokritos".
- Tselentis, G-Akis and Jiri Zahradnik (1999) Aftershock Monitoring of the Athens Earthquake of 7 September 1999. *Seis. Res. Let.*, 71, No. 3, pp 330-337.

Tumarkin, A.G. and R.J. Archuleta (1997) Recent Advances in Prediction and Processing of Strong Motions, *Natural Hazards*, 15, 199-215.

Voulgaris, N., I. Kassaras, P. Papadimitriou, and N. Delibasis (2000) Preliminary Results of the Athens September 7, 1999 Aftershock Sequence.

Wennerberg, (1983) " ... " BSSA Notes, Santa Barbara

Wu, F. T. and Ari Ben-Menahem (1965) Surface wave radiation pattern and source mechanism of the September 1, 1962, Iran earthquake. *Journal of Geophysical Research*, vol.70, no.16, pp.3943-3949, 1965.

Acknowledgments

This project was partially supported by the Lawrence Livermore National Laboratory, Campus/Laboratory Collaboration Project, and under the auspices of the U.S. Department of energy by the University of California, under contract No. W-7405-Eng-48. It was partially funded by Caltrans under contract #59A0238 for site response analysis.

Table 1: Stations (from Ioannidou et al., 2002)

Station	Latitude	Longitude	Location	Orient. I, t +90.0	No. events	Geol. categ	site specific t_g^*
ATHA ⁺	38.00°N	23.77°E	Neo Psihiko; 3-s reinforced concrete (RC); -13m	N180°E	16	c	.0031± .0002
ATHB ⁺⁺	37.93°	23.70°	Neo Faliro; Planetarium, 3-s RC	120°	4	c	.0025± .0012
COUR ^{**}	38.10°	23.65°	Fili, Soccer Stadium	0°	5	a	.0027± .0008
DEKL ⁺⁺	38.10°	23.78°	Dekelia, Air Base, 1-story	175° ⁺⁺	4	c	.0271± .0097
DFNA ⁺	37.95°	23.74°	Dafni; Metro station, -14m	155° ⁺⁺	1	c	.0086± ---
DMKA ⁺	37.99°	23.82°	Ag. Paraskevi; Research center, 1-story RC	135°	4	b	.0024± ---
FIXA ⁺	37.96°	23.73°	Sygrou-Fix; Metro station, -15 m	140°	4	c	.0046± ---
PEFK ^{**}	38.08°	23.62°	Thriassion plain, Ware House 1-story	0°	6	c	.0037± .0014
PNTA ⁺	38.00°	23.79°	Papagos; Metro station, -15m	135°	1	c	.0067± ---
RFNA ⁺	38.02°	23.99°	Private building, 1-s wood	250° ⁺⁺	1	b	.0048± ---
RNTA ⁺⁺	37.96°	23.68°	Rentis; Town Hall, 2-s RC	210°	3	c	.0075± ---
SGMA ⁺	37.98°	23.74°	Syntagma; Metro station, -7m	010°	7	b	.0051± .0014
SGMB ⁺	37.98°	23.74°	Syntagma; Metro station, -26m	135°	3	b	.0076± ---
SPLA ⁺	38.00°	23.71°	Sepolia; Metro station, -13m	320°	18	c	.0053± .0017
SPLB ⁺	38.00°	23.71°	Sepolia; Metro station, 3-s steel	320°	19	c	.0046± .0021
FILI ^{**}	38.12°	23.68°	Fili Monastery, free field	0°!	6	b	.0034± .0015
THVC ⁺	38.32°	23.32°	Thiva; Town Hall, 3-s RC	180°	5	b	.0027± .0016
PSAR ^{**}	38.09°	23.56°	Goritsa, house, ground fl, RC	0°	6	c	.0166± .0010
MAGO ^{**}	38.08°	23.52°	Magoula, 1-story RC	0°!	6	a	.0056± .0019
STEF ^{**} N00E bad	38.17°	23.55°	Stefani, Storage, ground fl, RC	0°!	5	b	.0111± .0032
ZOFR ^{**}	38.07°	23.69°	Zofria; free field	0°	6	a	.0026± .0011
NEOK ^{**}	38.05°	23.63°	Neokista ground fl, RC	0°!	6	a	.0024± .0007

+ NOAIG station

++ NOAIG, did not record main event

** Univ. of Athens data, did not record main event

*+ t component -90.0 from l component

! polarity may be reversed

Table 2: Geology of recording rites (from Ioannidou et al., 2002)

Site	Categ	Geology	Dist	Intensity*
ATHA	(c)	Tertiary deposits. 0-2m fill material, 2-6m poorly cemented conglomerate, 6-20m very weathered sandstone, 20-30m sandstone. (Attiko Metro, 1999)	25	V+, Filothei
ATHB	(c)	Holocene deposits. 0-1m soil, 1-8m brown sandy clay with pebbles, 8-12m brown stiff sandy clay, 12-20m brown stiff clay. (Geomihaniki E.P.E., 1999).	25	V+, Alimos; VI, Ag. Dimitrios
COUR	(a)	Middle Triassic - Lower Jurassic (Mesozoic). Dolomite-limestone formation, considerably fractured and folded. In the station area this formation overlies the Permian formation with a maximum thickness of 50 m.	18	VIII**
DEKL	(c)	Recent Deposits	24	VIII**
DFNA	(c)	Alluvium schist; 0-3.5m alluvial deposits, 3.5-9m Athenian schist - sandstone medium weathered, 9-30m Athenian schist - sandstone slightly weathered. (Attiko Metro, 1999)	26	V+, Agios and Dimitrios
DMKA	(b)	0-1m fill materials, 1-3m conglomerate altered to clayey sand gravel, 3-4m brown schist with many cracks and calcareous veins, 4-12m very humified peridoite, altered locally to clayey - loose or synectic - sand gravels. The site according to the New Seismic Resistant Code could be characterized as very altered rock sites, which are classified as granular soils from the engineering point of view (Tsamis, 1999).	29	V+, Vyronas
FIXA	(c)	Alluvium schist; 0-2m fill materials, 2-6.5m Athenian schist - calcareous siltstone, 6.5-11m Athenian schist - quartz siltstone, 11-14.5m siltstone and lime stone, 14.5-30m siltstone, calcareous siltstone and quartz siltstone. (Attiko Metro, 1999)	25	VII**
PEFK	(c)	Quaternary deposits	17	VII**
PNTA	(c)	Tertiary deposits; 0-3m fill material, 3-20m slightly cemented silty clay, 20-29m shales. (Attiko Metro, 1999)	26	V+, Filothei
RFNA	(b)	Tertiary deposits limestone	40	V, Lavrio; Keratea V+

Table 2: Geology of recording rites (from Ioannidou et al., 2002)

RNTA	(c)	Alluvium schist; 0-1.5m soil, 1.5-4m sandy siltstone, 4-7.5 brown clay, 7.5-13m mixture of sand, clay and silt, 13-15.5m sand, 15.5-20m sand and gravels, 20-23.5m stiff marl. (IoKede, 1981)	23	VI
SGMA	(b)	Schist; 0-12m Athenian schist - sandstone slightly weathered, 12-28m Athenian schist - sandstone slightly weathered and fractured. (Attiko Metro, 1999)	25	V+
SGMB	(b)	Schist; 0-12m Athenian schist - sandstone slightly weathered, 12-28m Athenian schist - sandstone slightly weathered and fractured. (Attiko Metro, 1999)	25	V+
SPLA	(c)	Alluvium schist; 0-6.5m fill material, 6.5-13.5m slightly cemented silty clay, 13.5-17m strongly cemented conglomerate, 17-22.5m sandy siltstone, 22.5-24m calcareous siltstone. (Attiko Metro, 1999)	22	VII
SPLB	(c)	Manmade deposits; 0-6.5m fill material, 6.5-13.5m slightly cemented silty clay, 13.5-17m strongly cemented conglomerate, 17-22.5m sandy siltstone, 22.5-24m calcareous siltstone. (Attiko Metro, 1999)	22	VII
FILI	(b)	Schist; Upper Palaeozoic (Permian). This formation consists of alterations of phyllites, sandstones, shales and graywackes, which appear significantly fractured folded and weathered, resulting to the existence of soil cover of important thickness. Due to the long history of tectonic deformation in the area, this formation is overthrust on the Triassic-Jurassic limestone formation.	19	VIII, Fili
THVC	(b)	Pleistocene deposits; 0-2m slightly cemented silty clay, 2-4m poorly cemented conglomerate, 4-6m strongly cemented conglomerate, 6-24m conglomerate (limestone pebbles in a reddish silty clay). (Edaphomihaniki E.P.E., 1998)	39	V, Thespies; V, Akrefinio; IV, Istiaia
PSAR	(c)	Neogene-Quaternary; Quaternary deposits of considerable depth, which mainly represents the product of erosion from the surrounding geological formations. Due to the unconsolidated nature and the sandy and silty character of these deposits this area can be characterized as a "soft" site	17	VII**

Table 2: Geology of recording rites (from Ioannidou et al., 2002)

MAGO	(a)	Limestone, Upper Cretaceous Limestone, uncomfortably overlies the dolomites and limestones of Mi-Triassic - Lower Jurassic.	18	VII**
STEF	(b)	Schist; Upper Palaeozoic (Permian). This formation consists of alterations of phyllites, sandstones, shales and graywackes, which appear significantly fractured folded and weathered, resulting to the existence of soil cover of important thickness. Due to the long history of tectonic deformation in the area, this formation is overthrust on the Triassic-Jurassic limestone formation.	20	VII**
ZOFR	(a)	Limestone, Middle Triassic - Lower Jurassic (Mesozoic). Dolomite-limestone formation, considerably fractured and folded. In the station area this formation overlies the Permian formation with a maximum thickness of 50 m.	19	VIII**
NEOK	(a)	Limestone; Lower Jurassic (Mesozoic). Dolomite-limestone formation, considerably fractured and folded.	18	VII**

*Intensities on the Modified Mercalli Scale calculated by the NOGIA for the main event (Kalogeras and Stavrakakis, 1999), and names of districts near the station where the intensity was evaluated

**Intensity values interpreted from isoseismals in Figure 3.

Table 3: Events used in the study (from Ioannidou et al., 2002)

Earthquake	Latitude	Longitude	Depth km	Ml	Mox10 ²¹ dyne-cm	fc Hz	mechanism STK DP SV	no. stat
1999/09/07 11:56:51*	38.08	23.58	16.8	5.4	94900	0.45	113° 39° -90°*	10
1999/09/07 11:59:10 ⁺	38.15	23.59	5.0**	***	228	3		6
1999/09/07 12:00:29 ⁺	37.92	23.78	17.8	***	176	2		6
1999/09/07 12:01:57 ⁺	38.07	23.75	5.0**	***	28.5	3		2
1999/09/07 12:03:54 ⁺	38.01	23.47	5.2	3.5 [!]	73 [!]	6		1
1999/09/07 12:05:12 ⁺	38.11	23.69	5.0**	***	228	2		4
1999/09/07 12:08:11 ⁺	37.82	23.71	5.0**	***	269	4		4
1999/09/07 12:16:10 ⁺	37.96	23.76	17.0	***	328	4		4
1999/09/07 12:20:25 ⁺	38.09	23.65	5.0**	***	344	5		1
1999/09/07 13:02:02 ⁺	38.07	23.62	5.0	***	26.3	4		2
1999/09/07 13:05:48 ⁺	38.13	23.51	18.2	***	322	3		1
1999/09/07 15:35:33 ⁺⁺	38.01	23.48	10.0	3.9	150	3		6
1999/09/07 15:42:52 ⁺⁺	38.07	23.45	3.0	3.5	72.8	6		1
1999/09/07 17:19:21*	38.11	23.72	16.2	3.8	260	3	114° 30° -87°	4
1999/09/07 20:44:55*	38.19	23.72	21.0	4.4	611	2		3
1999/09/08 03:21:32*	38.09	23.83	14.1	3.7	313	3		7
1999/09/08 03:35:20*	38.12	23.89	13.0	3.7	487	5	106° 30° -74°	3
1999/09/08 11:14:29 ⁺⁺	37.99	23.59	7.0	3.1	46.5	3		2
1999/09/08 12:55:01*	38.14	23.74	19.9	4.0	965	2	330° 70° -30°	2
1999/09/08 13:18:21*	38.08	23.81	9.2	3.7	99.8	3		4
1999/09/08 16:50:37*	38.19	23.91	1.4	3.6	185	4	113° 28° -67°	1
1999/09/08 16:54:08*	38.14	23.79	19.4	3.5	350	3	310° 50° -20°	1
1999/09/10 14:49:57 ⁺⁺	38.08	23.67	9.1	3.7	444	3	319° 70° -79°	10
1999/09/13 19:45:15 ⁺⁺	38.06	23.65	9.1	3.1	95.1	3	109° 50° -74°	11
1999/09/16 08:12:10 ⁺⁺	38.06	23.66	7.9	3.1	93.5	3	120° 54° -89°	11
1999/09/20 19:58:09 ⁺⁺	37.96	23.53	7.0	2.9	22.2	3		10
1999/09/20 20:17:25 ⁺⁺	37.97	23.64	8.8	2.9	2.90	7	250° 65° -48°	8
1999/10/03 17:03:34 ⁺⁺	38.09	23.75	9.0	3.5	252	3	159° 65° -48°	10
2000/03/23 03:09:18 ⁺⁺	38.08	23.74	15.0	3.5	412	3	120° 54° -89°	4

* location from Papadopoulos et al. (2000)

⁺ Location obtained from permanent networks in Greece and s-p arrival time intervals

⁺⁺ Solution from combined data of Univ. of Athens and National Observatory of Athens

⁺⁺ Locations routinely calculated by NOAIG from their permanent Greek network

^{**} Depth fixed

^{***} Magnitude obtained from moment/magnitude relationship

[!] Moment and magnitude obtained from spectral overlay with event 1999/09/07 15:42:52

Figures

Figure 1. The morphology of the Athens area, the epicenter of the main shock, and locations of stations and events used in this study (from Ioannidou et al., 2002).

Figure 2. Geology of the lower border area of Attica (modified from Katsikatsos et al., 1986), station locations, and epicenter of main event (from Ioannidou et al., 2002).

Figure 3. Isoseismal intensity from the earthquake in Modified Mercalli Scale, and individual intensity values for the same area as specified in Table 2 (from Ioannidou et al., 2002).

Figure 4. Plot of calculated site specific t_g^* values at each station. The circle size corresponds to t_g^* values (from Ioannidou et al., 2002).

Figure 5. Corrected spectra, as described in text, of all recordings for six events, and the fit of the simultaneous inversion for moment, source corner frequency, and individual station t_g^* (from Ioannidou et al., 2002).

Figure 6. Corrected spectra, as described in text, of all recordings for six events, and the fit of the simultaneous inversion for moment, source corner frequency, and individual station t_g^* (from Ioannidou et al., 2002).

Figure 7. Corner frequency values as a function of moment for the events in this study (triangles). and the corner frequency relationship predicted by a Brune source model with 100 bar stress drop (solid line) (from Ioannidou et al., 2002).

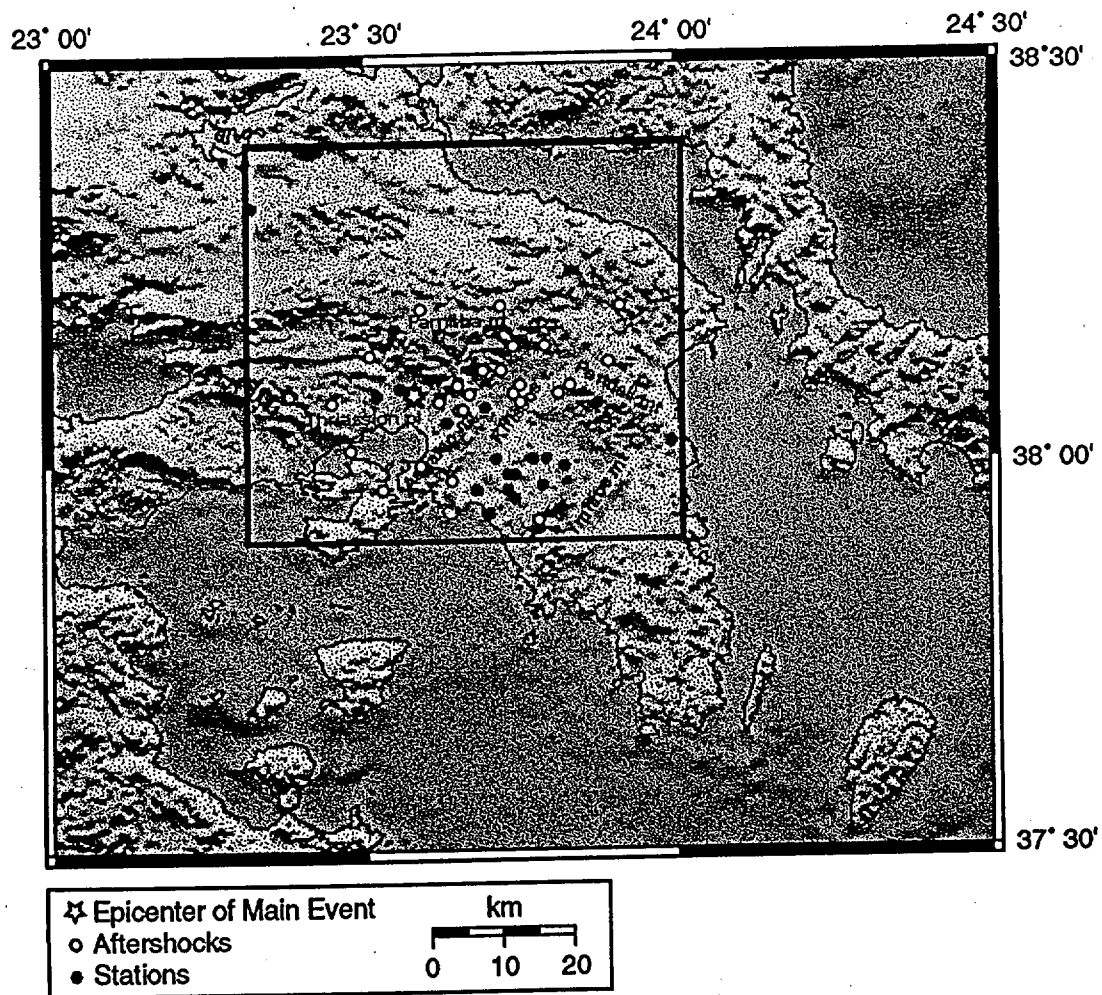
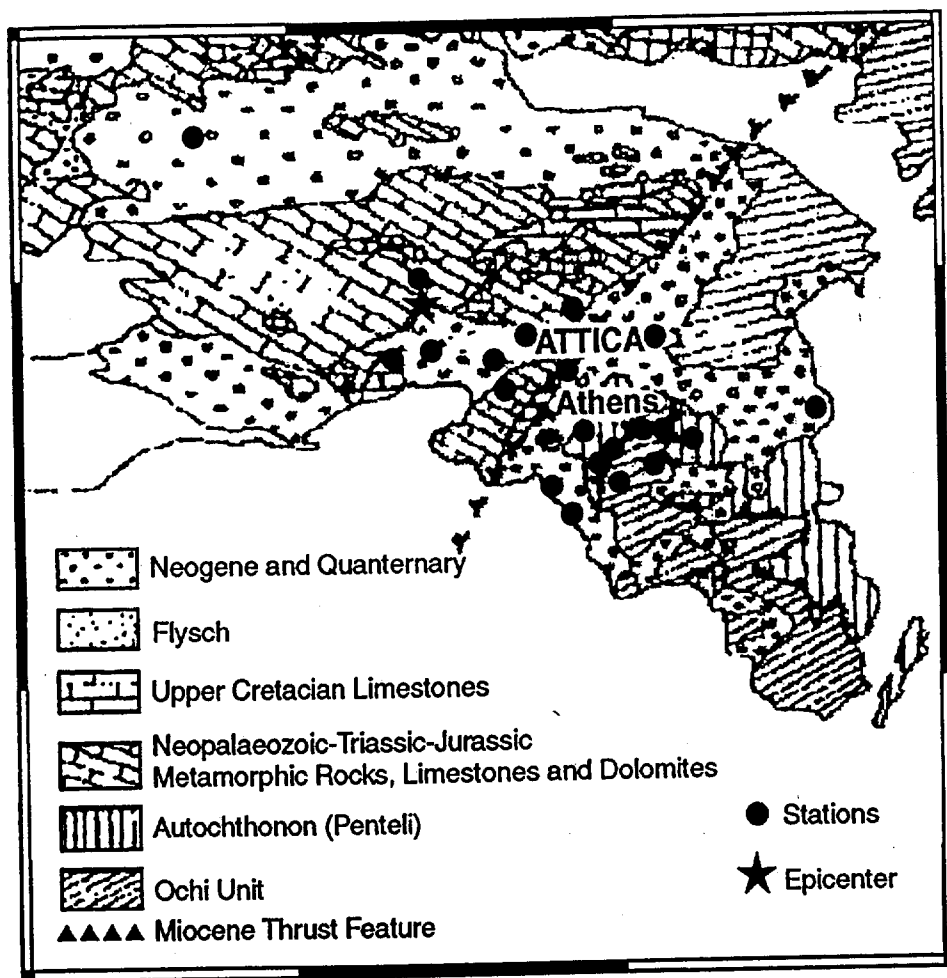


Figure 01
Hutchings



(Modified after Katsikatsos et al., 1986)

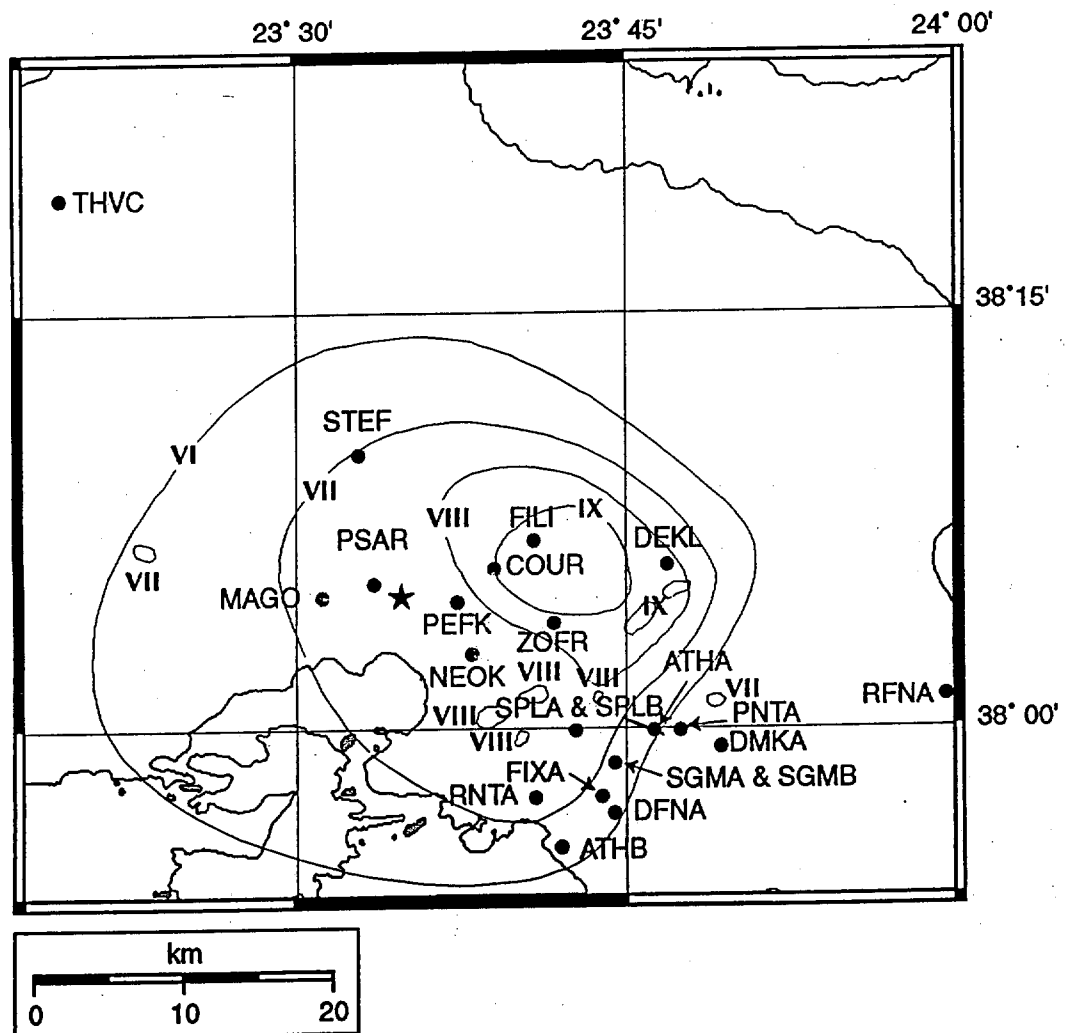


Figure 03
Hutchings

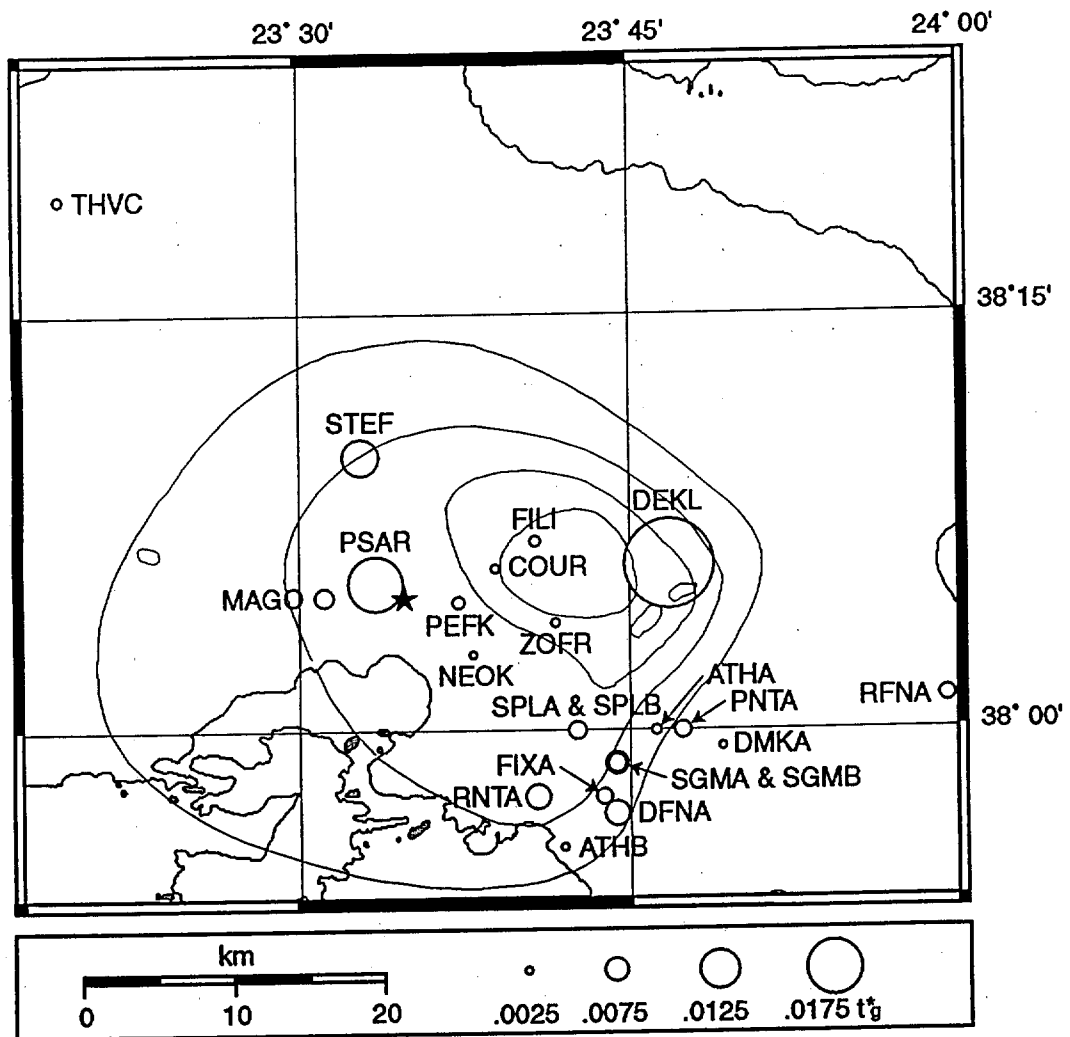


Figure 04
Hutchings

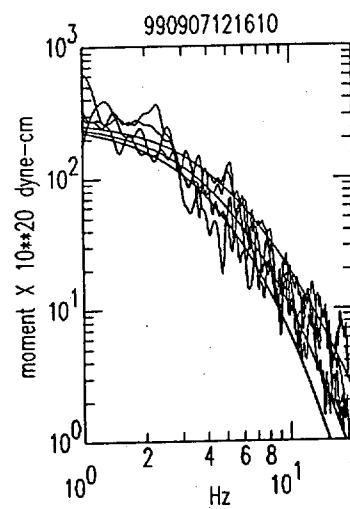
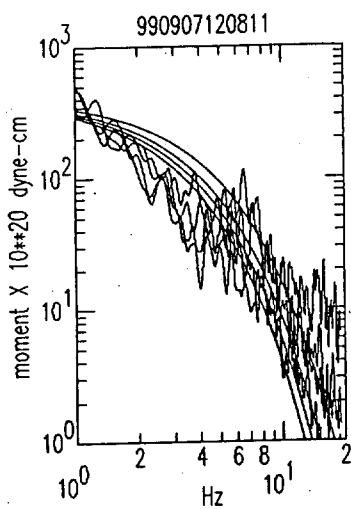
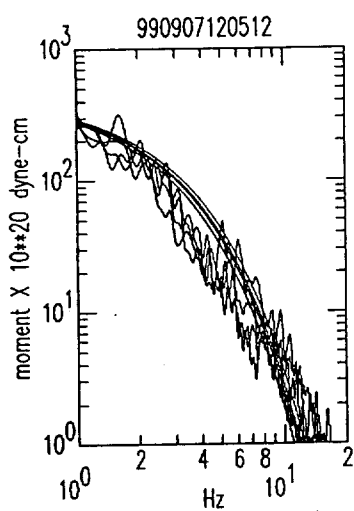
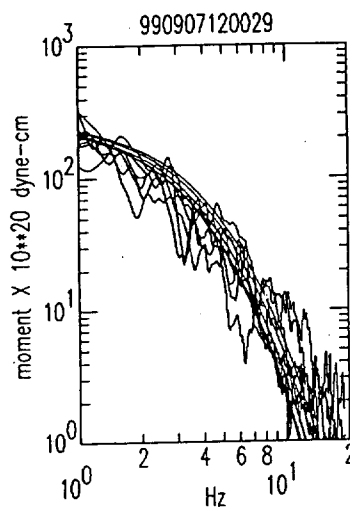
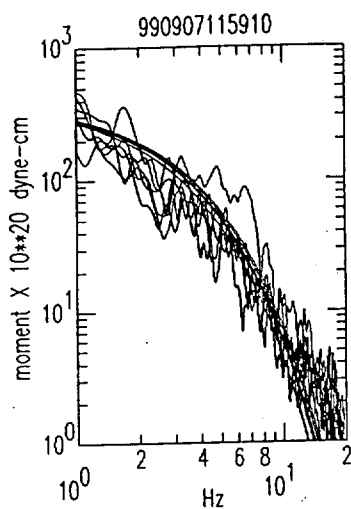
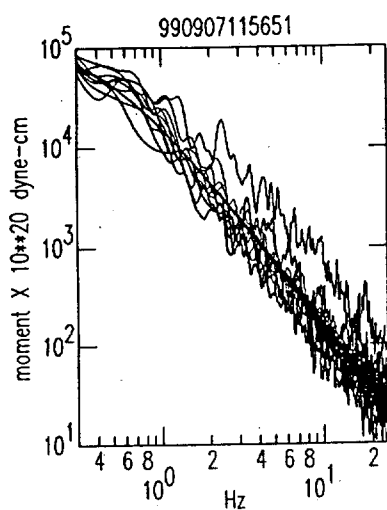


Figure 05
Hutchings

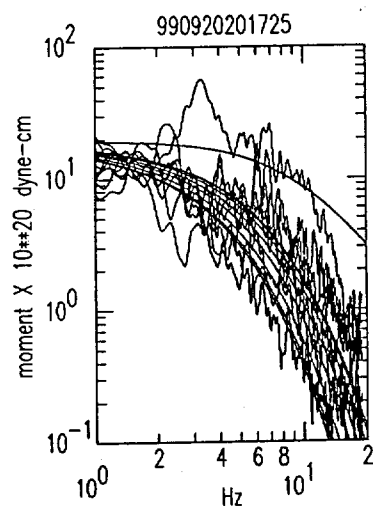
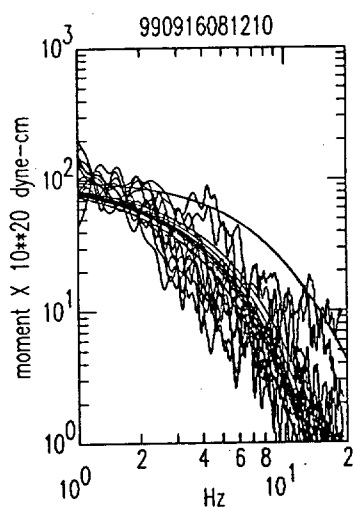
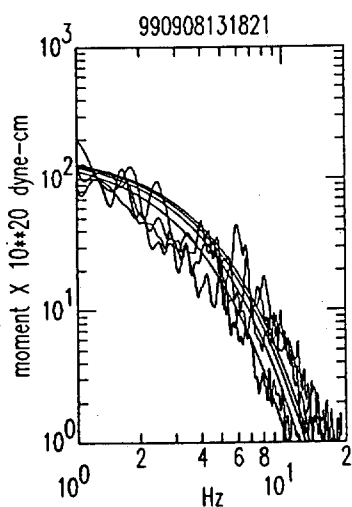
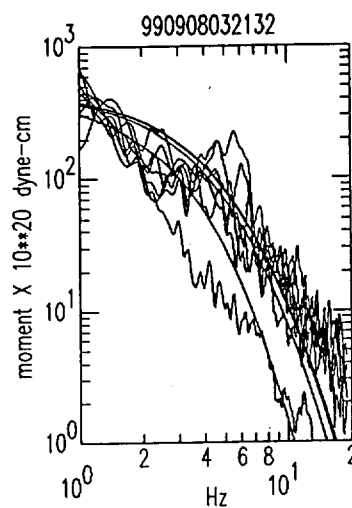
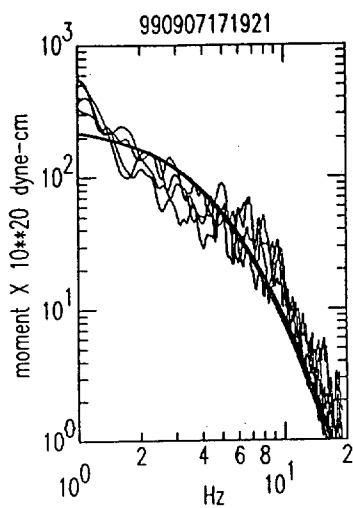
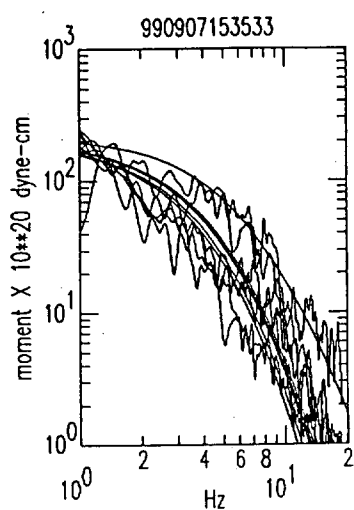


Figure 06
Hutchings

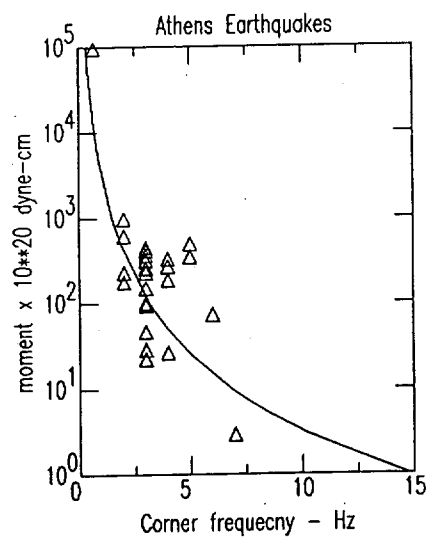


Figure 07
Hutchings

Appendix I

Program NetMoment

c Program NetMoment

c An individual or simultaneous inversion of recorded seismograms
c within a network to obtain event moment and corner frequency, and
c individual station t*.

c Lawrence Hutchings
c Hazard Mitigation Center
c University of California
c Lawrence Livermore National Laboratory

c This work was produced at the University of California, Lawrence
c Livermore National Laboratory (UC LLNL) under contract no.
c W-7405-ENG-48 (Contract 48) between the U.S. Department of Energy
c (DOE) and The Regents of the University of California (University)
c for the operation of UC LLNL. The rights of the Federal Government
c are reserved under Contract 48 subject to the restrictions agreed
c upon by the DOE and University as allowed under DOE Acquisition
c Letter 97-1.

c DISCLAIMER

c This work was prepared as an account of work sponsored by an agency
c of the United States Government. Neither the United States Government
c nor the University of California nor any of their employees, makes
c any warranty, express or implied, or assumes any liability or
c responsibility for the accuracy, completeness, or usefulness of any
c information, apparatus, product, or process disclosed, or represents
c that its use would not infringe privately-owned rights. Reference
c herein to any specific commercial products, process, or service by
c trade name, trademark, manufacturer or otherwise does not necessarily
c constitute or imply its endorsement, recommendation, or favoring by
c the United States Government or the University of California. The
c views and opinions of authors expressed herein do not necessarily
c state or reflect those of the United States Government or the
c University of California, and shall not be used for advertising or
c product endorsement purposes.

c NOTIFICATION OF COMMERCIAL USE

c Commercialization of this product is prohibited without notifying the
c Department of Energy (DOE) or Lawrence Livermore National Laboratory
c (LLNL).

program NetMoment

c Long period spectral levels (xarray) can be normalized to have average amplitude
c spectra. This is interpreted to account for uncertainties in spectral correction
c First, spectra are divided by avagm01, then multiplied by omega0. Trial for s
c is omega0 = avagm0fft.

c fmin is lowest frequency we can resolve,
c fmax is the highest frequency

parameter (maxdim=10000,maxstat=500,maxev=100)
parameter (tstar=0.05,fcstar=10.0)

c maxstat is three times the number of stations to allow for the three component
common /sres/ nfmmin,nfmax,smodel,resid,omega0,fc,tstar,fbeg,del,
*yarray
common /simul/ ttstar,ssmodel,ik,xarray,vss

```

complex tzaz(maxdim), tzar(maxdim), tzat(maxdim)
character*120 path,alpha,pathname(maxev),region,nnsf
character*20  cname(3),evname(maxev),nnsf1,nnsf2,revname
character*3   rdc,ans,ans1,ans2,jnt,decon,acomp,rec,nrmspc,wpth
character*4   cspp,cspt,blank,asbb,asb
real ma,mb
dimension yarray(10000),smodel(10000),resid(10000)
dimension y(maxstat),ttstar(maxstat),xarray(maxstat,maxdim),
*yarrayz(maxdim),yarrayr(maxdim),yarrayt(maxdim),slat(maxstat),
*slon(maxstat),traz(maxdim),trar(maxdim),trat(maxdim),asb(maxstat),
*spt(maxev),bdp(maxev),bsv(maxev),bm(maxev),ssmodel(maxstat,maxdim)
*,elat(maxev),elon(maxev),eh(maxev),bstr(maxev),amag(maxev),
*tral(maxdim),tra2(maxdim),tra3(maxdim),acomp(maxstat),pp(maxstat),
*avagmo(maxstat),bmo(maxev),bfc(maxev)
c need pp(maxstat) here because pp has different dimensions in simulspec and spe
data ans1,ans2/'yes','y'/

c
pi2 = 6.28318530717
pi = pi2/2.0
nrmspc = 'no'
open(12,file='NetMoment.out')
stime = 10.0
print*,'Do you want to deconvolve EGFs with a Brune source'
print*,'this is done after the moment calculation'
read(5,*) decon
3  print *, 'are records in acceleration (ACC), velocity (VEL), or dis
*placement (DIS)'
read(5,*) rec
if(rec.ne.'ACC'.and.rec.ne.'VEL'.and.rec.ne.'DIS') go to 3
call regionall(region,apz,vsp,vpm,zm,q,ma,mb)
136 format(//,'input velocity model: vp = ',f4.2,' + ',
*f4.2,'xH',//,'over half-space at ',f5.2,'km depth, with velocity ',
*f5.2//,'Q used for attenuation correction: ',f6.1//,'moment calculat
*ed from ',f5.2,' of S-arrivals; Sh and Sv'/'low frequency limit of
* the spectra',f4.1/'high frequency limit for inversion ',f5.1/
*'high frequency limit for fit to long period spectra ', f5.1/
*'starting value for tstar ', f6.4//)
print*,'file name for sources of Greens functions'
read(5,*) nnsf
open(10,file=nnsf)
print*,'file name for stations used in calculations'
read(5,*) nnsf
open(11,file=nnsf)
print *, ' '
print *, 'do you want joint inversion for t*, moment, and corner fr
*equency'
read(5,*) jnt
if(jnt.eq.ans1.or.jnt.eq.ans2) then
print *, 'joint inversion for corner frequency, moment and tstar'
print *, ' '
print *, 'do you want long period spectra levels to be normalized'
read(5,*) nrmspc
if(nrmspc.eq.ans1.or.nrmspc.eq.ans2) then
write(6,101)
write(12,101)
101 format('spectra normalized to have same long period amplitude for
*simultaneous inversion: omega0*xarray/avagmo1')
endif
else
print *, 'inversion for moment, fc, and tstar for individual statio

```

```

*ns'
endif
print *,''
print *,'do you want a whole path Q correction, from regionall.f'
read(5,*) wpth
print *,''
print *,'what is the low frequency limit of the spectra'
read(5,*) fmin
print *,''
print *,'what is the high frequency limit for fit to Brune model'
read(5,*) fmax
print *,''
print *,'what is the high frequency limit for fit to long period s
*pectra'
read(5,*) fmax1
print *,''
print *,'Do you want to make a radiation correction for'
print *,'difference between source events and elements'
read(5,*) rdc
write(6,16)
16 format(/,'Enter path for source event files')
read(5,'(a80)') path

```

c

```

write(6,136) vsp,apz,zm,vpm,q,stime,fmin,fmax,fmax1,tstrial
write(12,136) vsp,apz,zm,vpm,q,stime,fmin,fmax,fmax1,tstrial
if(rdc.eq.ans1.or.rdc.eq.ans2) then
if(bstr(ne).ne.0.0.or.bdp(ne).ne.0.0.or.bsv(ne).ne.0.0) then
print *,'radiation correction factor applied'
write(12,*) 'radiation correction factor applied'
endif
else
print *,'radiation correction factor of 0.63 utilized'
write(12,*) 'radiation correction factor of 0.63 utilized'
endif
if(rec.eq.'ACC') write(6,*) 'records integrated twice'
if(rec.eq.'VEL') write(6,*) 'records integrated once'
if(rec.eq.'DIS') write(6,*) 'records are in displacement'
if(rec.eq.'ACC') write(12,*) 'records integrated twice'
if(rec.eq.'VEL') write(12,*) 'records integrated once'
if(rec.eq.'DIS') write(12,*) 'records are in displacement'
do 100, ne = 1,maxev
read(10,*,end=1000) evname(ne),blank,elat(ne),elon(ne),eh(ne),
*amag(ne),bmo(ne),bfc(ne),bstr(ne),bdp(ne),bsv(ne)
if(evname(ne).eq.' ') go to 100
201 format(a20,1x,f9.4,1x,f10.4,1x,f5.2,3x,f3.1,1x,f6.1,1x,f4.1,1x,
*f6.1)
bdp1 = bdp(ne)*(pi2/360.0)
bsv1 = bsv(ne)*(pi2/360.0)
bstr1 = bstr(ne)*(pi2/360.0)
vzp = vsp+eh(ne)*apz
if(eh(ne).gt.zm) vzp = vpm
vzs = vzp/1.76
vss = vsp/1.76
c 'handbook on Mechanical Properties of Rocks', V II, R.D. Lama and V.S. Vutukur
c Trans Tech Publications, 1978, p. 245
den1 = sqrt((vsp - 0.35)/1.88)
den2 = sqrt((vzp - 0.35)/1.88)

```

c

c amag can be either magnitude or moment X 10**20
c conversion to moment

```
bmo(ne) = bmo(ne)*1.0e+20
```

c

c calculate moment from magnitude

```
bm(ne) = (10.** (ma*amag(ne) + mb))*1.0e+20
```

```
write(6,106) evname(ne),elat(ne),elon(ne),eh(ne),amag(ne),
```

```
*bmo(ne),bfc(ne),bstr(ne),bdp(ne),bsv(ne)
```

```
write(12,106) evname(ne),elat(ne),elon(ne),eh(ne),amag(ne),
```

```
*bm(ne),bfc(ne),bstr(ne),bdp(ne),bsv(ne)
```

```
106 format(//'*****New Event*****'/,a12,3x,  
*f7.4,2x,f9.4,2x,f5.2,1x,f3.1,1x,e12.4,1x,f4.1,2x,f4.0,3x,f3.0,2x,  
*f5.0)
```

```
write(6,103) den1**2,den2**2
```

```
write(12,103) den1**2,den2**2
```

```
103 format('surface density ',f4.2,' density at depth ',f5.2)
```

```
lentemp1 = indexb(path)
```

```
lentemp2 = indexb(evname(ne))
```

```
pathname(ne) = path(1:lentemp1)//'/'//evname(ne)(1:lentemp2)//'/'
```

```
lentemp3 = indexb(pathname(ne))
```

```
ik = 0
```

```
avagspec = 0.0
```

```
avagmofft = 0.0
```

```
amonet = 0.0
```

```
avagfc = 0.0
```

```
jstat = 0
```

```
do 50 j = 1,maxstat
```

```
avagmo(j) = 0.0
```

```
read(11,*,end=51) asbb,slatt,slonn,cname
```

```
if(asbb.eq.' ') go to 51
```

```
if(slatt.eq.0.0.or.slonn.eq.0.0) then
```

```
print *, 'need station information'
```

```
go to 50
```

```
endif
```

```
if(cname(1).ne.'.z'.and.cname(1).ne.'.zzz'.and.cname(1).ne.'.vz'.  
*and.cname(1).ne.'.v.sun') then
```

```
write(6,203) asbb
```

```
write(12,203) asbb
```

```
203 format('Station ',a4,' doesnt have first component at vertical')  
go to 50
```

```
endif
```

```
ik = ik + 1
```

```
asb(ik) = asbb
```

```
do 4 ji = 1,maxdim
```

```
traz(ji) = 0.0
```

```
trar(ji) = 0.0
```

```
trat(ji) = 0.0
```

```
tzaz(ji) = cmplx(0.0,0.0)
```

```
tzar(ji) = cmplx(0.0,0.0)
```

```
tzat(ji) = cmplx(0.0,0.0)
```

```
xarray(ik,ji) = 0.0
```

```
yarray(ji) = 0.0
```

```
yarrayz(ji) = 0.0
```

```
yarrayr(ji) = 0.0
```

```
4 yarrayt(ji) = 0.0
```

```
cspt = ' '
```

```
sptt = 0.0
```

```
lentemp4 = indexb(asbb)
```

```
nnsf = pathname(ne)(1:lentemp3)//asbb(1:lentemp4)//cname(1)
```

```
call rsac1(nnsf,traz,np,tim0,dt,maxdim,nerr)
```

```
c if (nerr.ne. 0) then
```

```
c ik = ik - 1
```

```

c      go to 50
c      endif
      call getfhv('T1', sptt, nerr)
      if (nerr .eq. 0) cspt = 'xx'
nnsf = pathname(ne) (1:lentemp3)//asbb(1:lentemp4)//cname(2)
      call rsac1(nnsf, trar, np, tim0, dt, maxdim, nerr)
      if (nerr .ne. 0) then
        ik = ik - 1
        go to 50
      endif
      if (cspt .ne. 'xx') then
        sptt = 0.0
        call getfhv('T1', sptt, nerr)
        if (nerr .eq. 0) cspt = 'xx'
      endif
      call getfhv('CMPAZ', rot1, nerr)
      if (nerr .ne. 0) then
        if (cname(2) .eq. 'n') rot1 = 0.0
        if (cname(2) .eq. 'e') rot1 = 90.0
      endif
      nnsf = pathname(ne) (1:lentemp3)//asbb(1:lentemp4)//cname(3)
      call rsac1(nnsf, trat, np, tim0, dt, maxdim, nerr)
      if (nerr .ne. 0) then
        ik = ik - 1
        go to 50
      endif
      if (cspt .ne. 'xx') then
        sptt = 0.0
        call getfhv('T1', sptt, nerr)
        if (nerr .eq. 0) cspt = 'xx'
      endif
      call getfhv('CMPAZ', rot2, nerr)
      if (nerr .ne. 0) then
        if (cname(3) .eq. 'n') rot2 = 0.0
        if (cname(3) .eq. 'e') rot2 = 90.0
      endif
      if (ik .ne. 1 .and. dt .ne. dtlast) then
        print *, 'all seismograms need to have the same sampling rate'
        stop
      endif
      dtlast = dt
      jstat = jstat + 1
      spt(jstat) = sptt
      slat(jstat) = slatt
      slon(jstat) = slonn
      nnsf1 = asbb(1:lentemp4)//cname(2)
      nnsf2 = asbb(1:lentemp4)//cname(3)
      call disazm(azm, azinv, dis, hdis, elat(ne), elon(ne), eh(ne),
        *slat(jstat), slon(jstat))
      write(12,147) asbb, slatt, slonn, hdis, nnsf1, rot1, nnsf2, rot2
      write(6,147) asbb, slatt, slonn, hdis, nnsf1, rot1, nnsf2, rot2
147  format(/'***station ',a4,f8.4,f11.4,' distance = ',f6.2/,'instrume
      *nt orientation for up on traces: '/,'traz UP'/', 'trar=',a6,' N',f4.0
      *, 'E'/', 'trat=',a6,' N',f4.0,'E'/', 'program rotates trar(i) into radi
      *al component and trat(i) into transverse component (trar + 90 deg
      *')

```

```

c
c rotate records into radial and transverse motions
do 200 jj = 1,np
  trarr = trar(jj)*cos((rot1-azm)*pi2/360.) +

```

```

      *trat(jj)*cos((rot2-azm)*pi2/360.)
      tratt = trar(jj)*cos((rot1-azm-90.0)*pi2/360. +
      *trat(jj)*cos((rot2-azm-90)*pi2/360.))
      trar(jj) = trarr
200  trat(jj) = tratt
c    call wsac1('tempr',trar,np,tim0,dt,nerr)
c    call wsac1('temptt',trat,np,tim0,dt,nerr)
c
      iss = ifix((spt(jstat)-tim0)/dt)
      write(6,424) spt(jstat),iss
      write(12,424) spt(jstat),iss
424  format('source event split for analysis ',f6.2,' sec from origin'
      *, ' iss = ',i4)
c
      lt = nint(0.5/dt)
      nt1 = nint((spt(jstat)-tim0-0.25)/dt)
      nt2 = iss + nint(stime/dt)
      kkk = 2*(nt2-nt1+2*lt)
      do 30 n = 1,100
      kk = 2**n
      if(kk.gt.kkk) go to 31
30  continue
31  signi = -1.0
c    call rtrend(traz,np)
c    call rtrend(trar,np)
c    call rtrend(trat,np)
      call rmean(traz,np)
      call rmean(trar,np)
      call rmean(trat,np)
      if(nt2.gt.maxdim) then
      print *, 'array elements exceed diemnsions, nmax in simulspec.f'
      stop
      endif
      call taper(np,nt1,nt2,traz,tzaz,n,lt,mp,mq,kk)
      call taper(np,nt1,nt2,trar,tzar,n,lt,mp,mq,kk)
      call taper(np,nt1,nt2,trat,tzat,n,lt,mp,mq,kk)
c spectra corrections done in taper
      call cool(n,tzaz,signi)
      call cool(n,tzar,signi)
      call cool(n,tzat,signi)
      del = 1.0/(float(kk)*dt)
      j1 = ifix(float(kk)/2. + 1.001)
      if(j1.gt.maxdim) then
      print *, 'maxdim too small'
      goto 1000
      endif
c
c cannot resolve frequencies shorter than the length of the record
c
      if(rec.eq.'DIS') go to 413
      call intg(tzaz,kk,dt)
      call intg(tzar,kk,dt)
      call intg(tzat,kk,dt)
      if(rec.eq.'VEL') go to 413
      call intg(tzaz,kk,dt)
      call intg(tzar,kk,dt)
      call intg(tzat,kk,dt)
c
c
c ccccccccccccccccccc

```

```

c
c compute radiation factor for source event
c
413 call linvel(eh(ne),dis,rp,angi,ainp,apz,vsp,vpm,zm,tt)
    bzmm = azm - bstr(ne)
    bzml = bzmm*(pi2/360.0)
    aangi = 360.*angi/pi2
    aainp = 360.*ainp/pi2
    ainsl = sin(ainp)/1.76
c roundoff accuracy
    if(ainsl.gt.1.0.and.ainsl.lt.1.05) ainsl = 1.0
    ains = asin(ainsl)
    vss = vsp/1.76
    aains = 360.*ains/pi2
c
    ffsv = sin(bsvl)*cos(2.*bdpl)*cos(2.*angi)*sin(bzml)-cos(bsvl)
    **cos(bdpl)*cos(2.*angi)*cos(bzml) + .5*cos(bsvl)*sin(bdpl)*
    *sin(2.*angi)*sin(2.*bzml) - .5*sin(bsvl)*sin(2.*bdpl)*
    *sin(2.*angi*(1.+sin(bzml)**2))
    if(ffsv.lt.0..and.ffsv.gt.-.25) ffsv = -.25
    if(ffsv.ge.0..and.ffsv.lt..25) ffsv = .25
    if(rdc.ne.ans1.and.rdc.ne.ans2) ffsv = 0.63
    if(bstr1.eq.0.0.and.bdp1.eq.0.0.and.bsv1.eq.0.0) ffsv = 0.63
c
    ffsh = cos(bsvl)*cos(bdpl)*cos(angi)*sin(bzml) +
    *cos(bsvl)*sin(bdpl)*sin(angi)*cos(2.*bzml)+sin(bsvl)*cos(2.*bdpl)
    **cos(angi)*cos(bzml) - .5*sin(bsvl)*sin(2.*bdpl)*sin(angi)*
    *sin(2.*bzml)
    if(ffsh.lt.0..and.ffsh.gt.-.25) ffsh = -.25
    if(ffsh.ge.0..and.ffsh.lt..25) ffsh = .25
    if(rdc.ne.ans1.and.rdc.ne.ans2) ffsh = 0.63
    if(bstr1.eq.0.0.and.bdp1.eq.0.0.and.bsv1.eq.0.0) ffsh = 0.63
c
    write(6,311) bzmm,bdp(ne),bsv(ne),aangi,aains,ffsv,ffsh
    write(12,311) bzmm,bdp(ne),bsv(ne),aangi,aains,ffsv,ffsh
311 format('fault-stat azi dip slip vector takeoff angle',
*' s incid angles',/6x,f6.1,5x,f4.1,4x,f6.1,13x,f5.1,12x,
*f4.1/'radiation factors sv sh',
*/24x,f6.3,3x,f6.3)
c
c scale spectrum to get moment calculation: radiation, distance, free surface co
c and moment factors
c
c free surface correction
c Aki and Richards p. 190
c
c p correction
c
    ampp1 = (1./vss**2 - 2.*rp**2)
    ampp2 = 4.*rp**2*cos(ainp)*cos(ains)/(vsp*vss)
    aampp = (ampp1**2 + ampp2)*vss**2*vsp/(-2.*vsp*cos(ainp)*ampp1)
c left hand coordinate
    aampp = -aampp
c
c sv correction
c
    aamsv = (ampp1**2 + ampp2)*vss**2/(2.*cos(ains)*ampp1)
c
c sh correction
    aamsh = .5

```

```

c
c exclude factor of 10**20
  facmor = abs(hdis*aamsv*4.*pi*den1*den2*vss**2.5*sqrt(vzs)/ffsv)
  facmot = abs(hdis*aamsh*4.*pi*den1*den2*vss**2.5*sqrt(vzs)/ffsh)
c
  do 120 k = 1,j1
    ws = float(k-1) * del
    if(ws.eq.0.0) ws = del
c undo correction for spectra from taper.f
    tzaz(k) = tzaz(k)*float(kk)*dt
    tzar(k) = tzar(k)*float(kk)*dt
    tzat(k) = tzat(k)*float(kk)*dt
    yarrayz(k) = facmor*sqrt(real(tzaz(k))**2 + aimag(tzaz(k))**2)
    yarrayr(k) = facmor*sqrt(real(tzar(k))**2 + aimag(tzar(k))**2)
    yarrayr(k) = sqrt(yarrayz(k)**2 + yarrayr(k)**2)
    if(wpth.eq.ans1.or.wpth.eq.ans2)
      *yarrayr(k) = yarrayr(k)*cmplx(exp(pi*ws*hdis/(q*vzs)),0.0)
c
    yarrayt(k) = facmot*sqrt(real(tzat(k))**2 + aimag(tzat(k))**2)
    if(wpth.eq.ans1.or.wpth.eq.ans2)
      *yarrayt(k) = yarrayt(k)*cmplx(exp(pi*ws*hdis/(q*vzs)),0.0)
c
  120 xarray(ik,k) = sqrt(yarrayr(k)**2 + yarrayt(k)**2)
c
c compute average spectral amplitudes from 1.0 to 10.0 Hz
c make correction for tstar (Q)
c
  alpha = asbb(1:lentemp4)//'_CorreSpec_'//evname(ne)(1:lentemp2)//
*'r'
  call wsac1(alpha,yarrayr,j1,0.0,del,nerr)
  alpha = asbb(1:lentemp4)//'_CorreSpec_'//evname(ne)(1:lentemp2)//
*'t'
  call wsac1(alpha,yarrayt,j1,0.0,del,nerr)
c
  i1 = ifix(fmin * float(kk)*dt + 1)
  i2 = ifix(fmax1 * float(kk)*dt + 1)
  if(maxdim.lt.i2-i1+1) then
    print *, '***** maxdim too small *****'
    go to 1000
  endif
c
  aavg1 = 0.0
  aavg2 = 0.0
  avagmol = 0.0
  do 15 i = i1,i2
    aavg1 = aavg1 + yarrayr(i)
    aavg2 = aavg2 + yarrayt(i)
  15 avagmol = avagmol + xarray(ik,i)
  aavg1 = aavg1/float(i2-i1+1)
  aavg2 = aavg2/float(i2-i1+1)
  avagmol = avagmol/float(i2-i1+1)
c compute moment
c
c
  avagmoo = sqrt(aavg1**2 + aavg2**2)
  avagmoo = avagmol*10.0**20
  write(6,317) avagmoo
  write(12,317) avagmoo
  317 format(/'moment from spectral amplitudes: '
*,e10.3)
c

```

```

nfmin = 1 + nint ( fmin/del )
nfmax = 1 + nint ( fmax/del )
fbeg = float(nfmin-1)*del

```

```

c
c trial for specfit, radial

```

```

omega0 = aavg1
fc = fctrial
tstar = tstrial
do 1001 i = 1,j1
  if(nrmspc.eq.ans1.or.nrmspc.eq.ans2) xarray(ik,i) = xarray(ik,i)/
  *avagmol
1001 yarray(i) = yarrayr(i)
  call specfit
  npts = nfmax-nfmin+1
  call newhdr
  call setnhv ('NPTS', npts, nerr)
  call setfhv ('B', fbeg, nerr)
  call setfhv ('DELTA', del, nerr)
  call setfhv ('USER0', omega0, nerr)
  call setfhv ('USER1', fc, nerr)
  call setfhv ('USER2', tstar, nerr)
  alpha = asbb(1:lentemp4)//'_BruneSpec_'//evname(ne)(1:lentemp2)//
  *'.r'
  call wsac1(alpha,smodel,npts,fbeg,del,nerr)
  amol = omega0
  fc1 = fc
  tstar1 = tstar

```

```

c
c trial for specfit, tangential

```

```

omega0 = aavg2
fc = fctrial
tstar = tstrial
do 1002 i = 1,j1
1002 yarray(i) = yarrayt(i)
  call specfit
  call newhdr
  call setnhv ('NPTS', npts, nerr)
  call setfhv ('B', fbeg, nerr)
  call setfhv ('DELTA', del, nerr)
  call setfhv ('USER0', omega0, nerr)
  call setfhv ('USER1', fc, nerr)
  call setfhv ('USER2', tstar, nerr)
  alpha = asbb(1:lentemp4)//'_BruneSpec_'//evname(ne)(1:lentemp2)//
  *'.t'
  call wsac1(alpha,smodel,npts,fbeg,del,nerr)
  amo2 = omega0
  fc2 = fc
  tstar2 = tstar

```

```

c
  avagfcc = (fc1+fc2)/2.0
  avagtstar = (tstar1 + tstar2)/2.0
  avagfc = avagfc + avagfcc
  avagmo(ik) = sqrt(amol**2 + amo2**2)*10.**20.0
  write(6,318) avagmo(ik),avagfcc,avagtstar
  write(12,318) avagmo(ik),avagfcc,avagtstar
318 format('moment from specfit output: '
  *,e10.3,' corner freq ',f5.2,' tstar ',f6.5)
  avagspec = avagspec + alog10(avagmo(ik))
  avagmofft = avagmofft + avagmol
50 continue

```

```

51  rewind(11)
    avagspec = 10.0**(avagspec/float(ik))
    avagmofft = avagmofft/float(ik)
    avagfc = avagfc/float(ik)
    if(ik.lt.2) go to 100
    if((ik+3)*(ik+2).gt.maxstat) then
    write(6,53) ((ik+3)*(ik+2)), maxstat
53  format('(ik+3)*(ik+2)=' ,i6, ' maxstat= ',i5)
    print *, 'maxstat too small'
    go to 1000
    endif
c trial for simulspec
    fc = avagfc
    omega0 = avagmofft
    if(nrmspc.eq.ans1.or.nrmspc.eq.ans2) omega0 = 1.0
    tstar = ttrial
    if(jnt.eq.ans1.or.jnt.eq.ans2) then
    print *, ' '
    print *, 'call simulspec'
    call simulspec(pp)
    if(nrmspc.eq.ans1.or.nrmspc.eq.ans2) then
    omega0 = omega0*avagmofft
    amonet = omega0*(10.**20.0)
    do 1004 j = 1, ik
    do 1003 i = 1, j1
    ssmodel(j,i) = ssmodel(j,i)*avagmofft
1003 xarray(j,i) = xarray(j,i)*avagmofft
1004 continue
    avagmofft = avagmofft*10.**20.0
    endif
c
c Brune Stress drop in kilobars, 1 bar = 10**6 dyne/cm**2
    str = ((7./16.)*amonet*(pi2*fc/(2.34*vzs*10.0**5.))**3.)*
    *10.0**-3.
    do 150 k = 1,ik
    if(ttstar(k).lt..00001) ttstar(k) = .00001
    asbb = asb(k)
    call newhdr
    call setnhv ('NPTS', npts, nerr)
    call setfhv ('B', fbeg, nerr)
    call setfhv ('DELTA', del, nerr)
    call setfhv ('USER0', omega0, nerr)
    call setfhv ('USER1', fc, nerr)
    call setfhv ('USER2', ttstar(k), nerr)
    do 250 j = 1,npts
    yarray(j) = xarray(k,j)
250  smodel(j) = ssmodel(k,j)
    alpha = asbb(1:lentemp4)//'_NetMoment_'//evname(ne)(1:lentemp2)
    call wsac1(alpha,smodel,npts,fbeg,del,nerr)
    alpha = asbb(1:lentemp4)//'_NetCorrec_'//evname(ne)(1:lentemp2)
    call wsac1(alpha,yarray,npts,0.0,del,nerr)
150  continue
    endif
    varmo = 0.0
c variance of mean is 1/ik variance of population
c since differences are calculated in log space they are rations, so that
c results are a facotr.
    do 205 i = 1,ik
205  varmo = varmo + (alog10(avagspec)-alog10(avagmo(i)))**2
    varpop = 10.**sqrt(varmo/float(ik-1))

```

```

varmean = varpop/float(ik)
varmean = avagspec*varmean
varpop = avagspec*varpop
write(6,202) evname(ne),bmo(ne),bfc(ne),amag(ne),bm(ne),avagmofft,
*avagspec,avagfc,amonet,varmean,varpop,fc,(asb(i),ttstar(i),
*(1.0/(ttstar(i)*vss)), i=1,ik)
write(12,202) evname(ne),bmo(ne),bfc(ne),amag(ne),bm(ne),avagmofft
*,avagspec,avagfc,amonet,varmean,varpop,fc,(asb(i),ttstar(i),
*(2.0/(ttstar(i)*vss)), i=1,ik)
202 format(//'****Network Moments***** ',a12//,'moment from sources fi
*le :',e12.4,', corner freq:',f5.1/,'magnitude: ',f3.1,', moment fr
*om moment/mag rel:',e12.4/'Log-Normal Average from peaks of spectr
*al amplitudes: ',e10.3/,'Log-Normal Average from individual Specfi
*t runs:',e10.3,', corner frequency ',f6.2/,'Simultaneous solution f
*or all components: ',e10.3,', variance of mean ',e10.3/,'variance
*of population ',e10.3,', corner frequency ',f6.2/'station tstar
* Q (R=2.0km) '/, (2x,a4,5x,f6.4,4x,f7.0))
100 continue
C
1000 close(10)
close(11)
close(12)
stop
end

```